DESIGN OPTIMIZATION OF A COMPLEX MECHANICAL SYSTEM USING ADAPTIVE RESPONSE SURFACE METHOD

G. Gary Wang
Assistant Professor
Department of Mechanical and Industrial Engineering
University of Manitoba

Zuomin Dong
Professor
Department of Mechanical Engineering
University of Victoria

ABSTRACT

Today's increasingly competitive industrial environment demands shorter product development lead-times, lower costs, and higher quality products. These requirements produce more complex design problems that are characterized by multiple design objectives as well as complex design objective and constraint relations. The optimization of these computationally intensive design problems leads to new technical challenges. This work applies a new global optimization search scheme, the Adaptive Response Surface Method (ARSM), to the optimal design of a complex mechanical system -- the radiator stack PEM fuel cell system. The design optimum manifests a significant increase in system performance and decrease in cost. The proposed method can also be applied to the solution of other complex design optimization problems.

Keywords: *Design Optimization, Engineering Design, Response Surface Method, Virtual Prototyping, and Fuel Cell System.*

OPTIMIZATION DU CONCEPT D'UN SYSTÈME MÉCANIQUE COMPLEXE PAR LA MÉTHODE DE SURFACE À RÉPONSE ADAPTIVE

L'environnement industriel de plus en plus compétitif qui pévaut de nos jours, éxige des délais de développement de plus en plus courts, des coûts réduits, ainsi qu'une amélioration de la qualité. Ces besoins mènent à des problèmes de conception plus complexes, caracterisés par des objectifs de conception multiples ainsi que des fonctions de contraintes complexes. L'optimization de ces problèmes de conception nécéssite des calculs numériques intensifs et mène à de nouveaux défis techniques. Dans cet article, nous appliquons un nouveau schéma d'optimization globale, la méthode de surface à réponse adaptive (ARSM). Cette méthode est appliquée a un système mécanique complexe: la pile a combustible PEM basée sur le concept de radiateur. L'optimization du concept de base résulte en une amélioration substantielle de la performance et une diminution du coût du système. La méthode peut être également appliquée pour la résolution d'autres problèmes complexes de conception-optimization.

INTRODUCTION

With the advance of Computer-Aided Design (CAD), Computer-Aided Engineering (CAE) and virtual reality software, virtual prototyping technique are emerging as a new tool that is used by leading manufacturing industry to shorten product development lead-times and to meet the challenges from today's competitive industrial environment.

Virtual prototyping involves two major tasks: (a) the construction of a "soft prototype" of the design using a CAD system, and (b) the "tests" on the soft prototype through various analyses, simulations, and evaluations using CAE tools, as if they would be performed physically on a physical prototype. Expert feedbacks are also included. These are carried out by the specialists on the difficult-to-evaluate product performance issues, such as manufacturability, maintainability, service-ability and appearance. With virtual prototyping, numerous design tests can be quickly made for various product configurations without the lengthy and costly physical prototyping process. The number of necessary physical prototypes can be radically reduced [1][8]. At present though virtual prototyping can give an accurate prediction of product performances, a designer has to manually go through the design-evaluation-redesign process many times before a satisfactory solution is achieved. An ideal approach is to use virtual prototyping as product performance evaluation means and to optimize the design based upon these evaluations. However, virtual prototyping involves computationally intensive and time-consuming processes and results in complex optimization problems with multiple design objectives and complex design functions.

Numerical optimization is a powerful tool in search of the best design solution [6], and a large number of optimization algorithms have been developed for a single-modal objective function. As today's industrial designs are usually complex and multi-objective, resulting in multi-modal objective functions, conventional optimization methods often stop at local design minima [17]. Global optimization algorithms with both deterministic and probabilistic methods are used to handle these multi-modal problems. However, these methods cannot be directly used in virtual prototyping-based design optimization. Most present deterministic global optimization methods require the knowledge on the forms of the design objective and constraints [7][10][11]. While virtual prototyping is carried out using implicit computer models and software tools, explicit design objective and constraint functions are often unavailable. Two probabilistic global optimization algorithms, *Simulated Annealing (SA)* and *Genetic Algorithms (GA)*, are widely used today due to their good reliability. Both of these two methods, however, need a large number of design function evaluations[4][30]. The numerous iterations required in their search make them computation intensive procedures and preclude their use in combination with the computation intensive virtual prototyping process. Consequently, a new design optimization method is needed to efficiently carry out the search for the global optimum in these complex design optimization problems.

Designs of Experiment (DOE) methods are used to explore unknown systems and implicit design objectives. The *Response Surface Method* (RSM) is one of the DOE schemes to approximate and simplify design optimization problem [3][13][19][18][26]. The method is suitable for problems in which the system output is influenced by several variables and the design objective is to optimize the output, or system response. Recently, RSM were broadly applied to the approximation of complex objective and constraint functions [4][12][9] [22][15].

The RSM is based on a series of planned experiments. A first or second-order regression model is used to fit the experimental points to approximate the unknown or complex relationship between design variables and design functions. This approach approximates the unknown system through only one pass. It is thus regarded as *one-time RSM* in this work. If one considers a virtual prototyping process as a simulation of a physical experiment, RSM bears a number of appealing

features for the virtual prototyping-based design optimization. These include supporting distributed computation, providing explicit function expression and variable sensitivities, and allowing both continuous and discrete design variables [9]. Nevertheless, the present *one-time RSM* has two major limitations:

- It is difficult to determine the appropriate experimental designs for the response surface fitting.
  The response surface obtained from regression depends upon the number and distribution of the experimental designs. The selection of design experiments is case dependent to the function to be approximated. The *one-time RSM* cannot ensure an adequate fitting for some design problems due to its one-size-for-all nature.
- The response surface model cannot adequately represent a high-order design function.
  One-time RSM uses a first or second order regression model to approximate a complex design function that is often in a higher order form, leading to significant modeling errors over the design space.

These limitations undermine the creditability of the obtained response surface and the design optimum. To overcome these problems, the *Adaptive Response Surface Method* (ARSM) was introduced in the authors' recent work [27][30][28]. The approach extended *one-time RSM* by eliminating the two stated drawbacks, and made virtual prototyping based design optimization feasible.

ADAPTIVE RESPONSE SURFACE METHOD

Description of the ARSM Algorithm

1. Carrying out design experiments to produce a data set of design variables and the corresponding function values.
   A formal experimental design method, e.g. Central Composite Design (CCD), is applied to explore the unknown design space with normalized variables [18].
2. Building a second-order approximation model of the design function using data in the design experiment data set and the least square method.
3. Calculating the optimum of the fitted response surface and updating the experimental designs.
   The optimum of the fitted model is obtained using the *simulated annealing* method. The use of this global optimization method allows a complex problem with nonlinear constraints to be handled with confidence. The design function value at the optimum of the approximation model is calculated through an evaluation of the original design function. If this estimated optimum presents a better solution than all other probe points in the design experiments, the point is added to the set of experimental designs for the following iteration as this point represents a promising search direction.
4. Reducing the design space using a threshold according to the function value of experimental designs in the data set and the correlation of design variables.
   Part of the original design space in which the function values of possible design points are higher than the threshold is discarded. In this algorithm, the second highest value of the design function in the set of experimental designs is chosen as the cutting plane. If this second highest value of the design function cannot help to reduce the design space, the next highest value of the design function will be chosen, and so on.
5. Stop when a satisfactory design appears in the design library or the design space cannot be further reduced. Otherwise, go to Step 1 with the reduced design space.

Reduction of the Design Space

Within each ARSM iteration, the design space is continuously reduced, given the cutting plane and the fitted function. Identification of the reduced design space for a generic, multiple-variable design problem is carried out through an optimization on the fitted model:

$$y = \beta_0 + \sum_{i=1}^{n} \beta_i x_i + \sum_{i=1}^{n} \beta_{ii} x_i^{\,2} + \sum_{i,i<j} \sum_{j}^{n} \beta_{ij} x_i x_j \quad (1)$$

where the β_i and β_{ij} represent regression coefficients; $x_i, (i = 1 \cdots n)$ are design variables and y is the response. Given a design threshold, y_0, the possible solutions for x_k, can be calculated by:

$$x_{k,1}, x_{k,2} = \frac{-b \pm \sqrt{b^2 - 4ac}}{2a}, \quad a \neq 0 \qquad (2)$$

where

$$a = \beta_{kk}$$

$$b = \beta_k + \sum_{i=1,\neq k}^{n} \beta_{ik} x_i$$

$$c = \sum_{i=1,\neq k}^{n} (\beta_{ii} x_i^2 + \beta_i x_i) + \sum_{\substack{i=1,\neq k \\ i<j}}^{n} \sum_{j=1,\neq k}^{n} \beta_{ij} x_i x_j + \beta_0 - y_0$$

The lower limit of x_k is identified by

Minimize

$$\min \{x_{k,1}, x_{k,2}\} \qquad (3)$$

subject to

$$x_{lower,i} \leq x_i \leq x_{upper,i} \quad i = 1, \cdots k-1, k+1, \cdots n \qquad (4)$$

The upper limit of x_k is identified by

Minimize

$$-\max \{x_{k,1}, x_{k,2}\} \qquad (5)$$

subject to

$$x_{lower,i} \leq x_i \leq x_{upper,i} \quad i = 1, \cdots k-1, k+1, \cdots n \qquad (6)$$

DESIGN OPTIMIZATION OF A COMPLEX MECHANICAL SYSTEM

ARSM is introduced to solve an ill-shaped, complex design optimization problem that requires extensive computation in evaluating its objective and constraint functions. The method applies an iterative process to progressively improve the approximation to the unknown design function using a second-order polynomial response surface model, thus not relying on the initial selection of experimental designs. As the design space is reduced, the response surface can accurately represent a high-order design function in a sufficiently small region. The method has been extensively tested using benchmark problems, and applied to a number of industrial design problems [27,28,30]. In this work, the optimal design of a complex mechanical system - the transportation fuel cell system is presented.

A Fuel Cell

A fuel cell is an electric power-generating element based on the controlled reaction of fuel and oxidant. A typical fuel cell is illustrated in Fig. 1, in which hydrogen is shown as the fuel and oxygen as the oxidant.

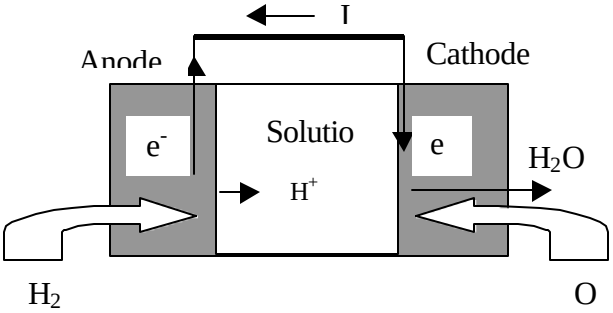

Fig. 1 Illustration of a fuel cell

The overall reaction equation is:

$$H_2 + \frac{1}{2} O_2 \rightarrow H_2O + Heat + Electrical\ Potential \qquad (7)$$

In principle, fuel cells are more efficient in energy transfer and much cleaner than internal combustion engine [16]. Due to many attractive features such as low temperature, compact structure, and less corrosion concern, the proton exchange membrane (PEM) fuel cell has received increasing attentions, especially in the automotive industries. A PEM fuel cell forms the basic element of a transportation fuel cell system. Dozens of fuel cells are bundled together to form a modular power unit, the fuel cell stack. To satisfy the need of a stationary power plant or to serve as the power source of a vehicle, multiple fuel cell stacks are connected. Together with ancillary components, these fuel cell stacks form a fuel cell system.

The operation of a fuel cell involves very complex mass transfer processes. The performance of a fuel cell cannot be considered in isolation of the stack and the system. Design optimization, if conducted, has to be carried out at a stack and system level to optimize the performance and minimize the costs of fuel cells as an "engine" or "generator." The fuel cell stacks also have to satisfy structural integrity requirements and the fuel cell system has to meet the space constraint of a vehicle for the transportation application.

As the high cost of transportation fuel cells hampers its commercialization, the task of fuel cell system design is thus to lower the cost while maintaining high functional performances. While the fuel cell system cost is highly interlaced with the system performance, the design problem represents a real challenge to the design optimization. This work applies virtual prototyping to simulate the fuel cell performances and calculate the system cost of a new stack design, the Tri-stream, External Manifolding, and Radiator Stack (TERS), and its fuel cell system. The ARSM is used to perform the design optimization.

Integrated Modeling of System Performances and Costs

The TERS fuel cell system configuration is illustrated in Fig. 2. Its system model is based on the work of [20] with the following modifications:

- Improvement of the cell performance model from pure empirical to a model with both theoretical and empirical bases. The pure empirical cell performance model can only give a fixed performance reading for a given design, while the improved model can reveal the internal relations among design variables and system performance.
- Development of a cost model for the TERS fuel cell system, and
- Integration of the performance and cost models.

The central components of the TERS fuel cell system are the TERS stacks. The function and configuration of the stacks determine ancillary components. The configuration of the stack is illustrated in Fig. 2.

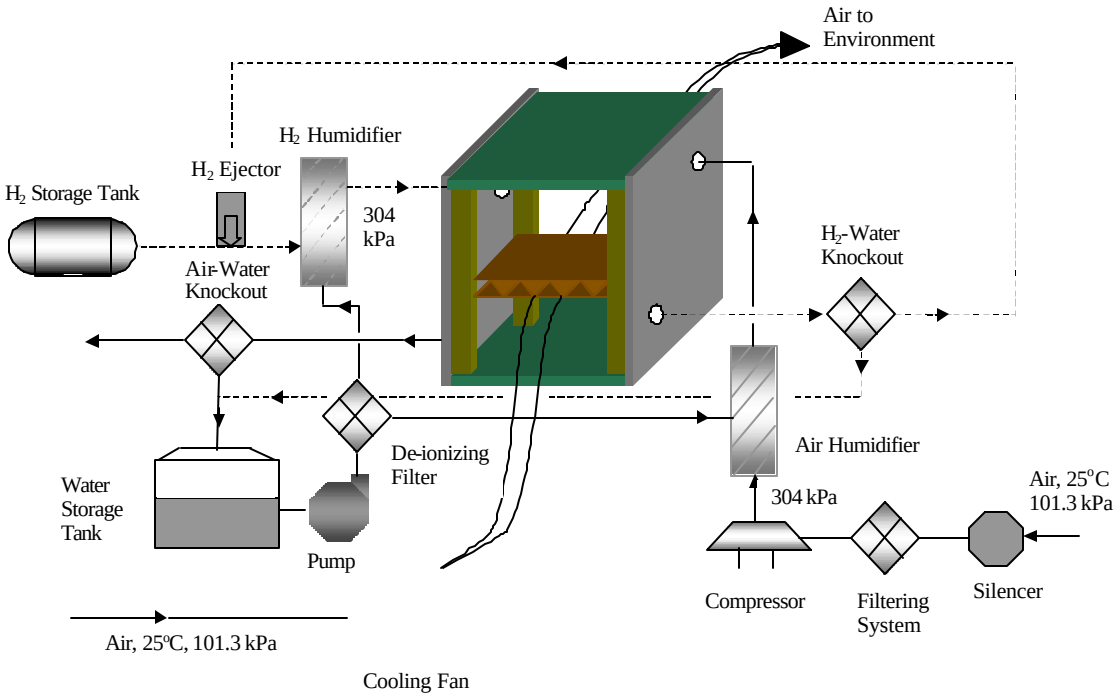

Fig. 2 Schematic Layout of TERS Fuel Cell System

System Performance Model

The cell performance is evaluated based on a few widely accepted assumptions [14][1]. These include

- The proton exchange membrane used in TERS is Nafion 117™, which has a good reliability and published property data.
- The fuel cell operates at around 85°C, where Nafion 117™ gives the best performance.
- The reactant pressure, *P*, is 3 bars for both hydrogen and air. This value is given by Amphlett based on experiments on Nafion 117™.
- The membrane is fully hydrated to maintain a normal performance.

As the cell conditions used in the model are close to the benchmark Ballard Mark IV stack, the thermodynamic potential of the fuel cell reaction thus can be described using the same mechanistic formula [1]:

$$E_{theory} = 1.229 - 0.00085(T - 298.15) + 0.000043085\,T[\ln(P_{H_2}^{Interface}) + 0.5\ln(P_{O_2}^{Interface})] \quad (8)$$

where, $P_{H_2}^{Interface}, P_{O_2}^{Interface}$ are the partial pressures for hydrogen and oxygen along the channel, respectively. T is the fuel cell operating temperature. Amphlett also gave formulas for the activation potential and ohmic potential losses obtained by fitting empirical data of fuel cells using pure oxygen. In this work, the model parameters are determined using data from an ambient air system.

The fitted voltage loss and the resultant cell voltage formulas are

$$E_{activation} = -0.944 + 0.00354T + 0.0000785T\ln(C_{O_2}^*) - 0.000196T\ln(I) \quad (9)$$

$$E_{ohmic} = -I(0.0033 - 0.00000755T + 0.0000011I) \quad (10)$$

$$V = E_{theory} - E_{activation} - E_{ohmic} \quad (11)$$

where, I is the total current, and $C_{O_2}^*$ is the oxygen concentration, calculated by [1].

$$C_{O_2}^* = \frac{P_{O_2}^{Interface}}{5.08 * 10^6 e^{(\frac{-498}{T})}} \quad (12)$$

$$P_{O_2}^{Interface} = P[1 - x_{H_2O}^{sat} - x_{N_2}^{channel} e^{(\frac{0.291I}{T^{0.832}})}] \quad (13)$$

$$P_{H_2}^{Interface} = P[1 - 0.5x_{H_2O}^{sat}] \quad (14)$$

where, $x_{H_2O}^{sat}, x_{N_2}^{channel}$ are the mole fraction of water and nitrogen among the gas stream, respectively. For the water vapor, its saturation pressure is only a function of the cell temperature. It can be defined using empirical equation [5].

$$\ln(P_{sat}) = 70.434643 - 7362.6981/T + 0.006952085\,T - 9.0000\ln T \quad (15)$$

where, T is temperature in Kelvin and P_{sat} is the saturation pressure in atmosphere. With the water saturation pressure known, the mole fraction of water along the flow channel can be obtained as

$$x_{H_2O}^{sat} = \frac{P_{sat}}{P} \quad (16)$$

The nitrogen mole fraction is the log mean average mole fraction in the humidified gas at the inlet and the outlet of the gas flow channel.

$$x_{N_2}^{in,hum} = (1 - x_{H_2O}^{sat}) * 0.79 \quad (17)$$

$$x_{N_2}^{out,hum} = \frac{1 - x_{H_2O}^{sat}}{1 + \frac{stoiAir - 1}{stoiAir}\frac{0.21}{0.79}} \quad (18)$$

The rest of the fuel cell system modeling, including the heat and mass balance, follows the work of [20]. The performance simulation involves many recursive procedures and non-linear functions. The relation between design variables and performance output is hidden in these complex and computation intensive processes.

System Cost Model

The total cost of the TERS fuel cells system, *C*, is calculated by

$$C = N_{stack}C_{stack} + C_{H_2} + C_{Air} + C_{cool} + C_{control} \quad (19)$$

where, N_{stack} is the number of stacks and the five *C* terms represents the cost of each stack, the cost of the hydrogen supply module, the cost of the air supply module, the cost of the cooling module, and the cost of the control module, respectively. The costs of the hydrogen and air supply modules are calculated based upon the sum of fixed costs for each system and the cost of gas consumption. The control and cooling unit cost is chosen as a fixed value given in [23]. Due to the embedment of the radiator in the stack, the cost of cooling panels is taken into account in the stack cost. The number of stacks is determined by the gross power output divided by the gross power output per stack. The stack cost is calculated by

$$C_{stack} = N_{cell}C_{cell} + C_{endplt} + C_{column} + C_{mani} + C_{panel} + C_{assem} \quad (20)$$

where, N_{cell} is the number of fuel cells per stack; C_{cell} is the fuel cell cost; C_{column} , C_{mani} , and C_{panel} are the material and manufacturing cost for the supporting columns, manifolds, and the cooling panels, respectively (See Fig. 2). C_{assem} is the stack assembly cost.

$$C_{cell} = C_{mea} + 2C_{dplt} + C_{overhead} \quad (21)$$

where, C_{mea}, C_{dplt}, and $C_{overhead}$ are the cost for membrane electrode assembly (MEA), delivery plates, and overheads, respectively. The cell cost is a function of geometric variables such as the stack width, column width, and so on. The cost for delivery plates is estimated based on the screen printing technique developed within the RSA research group [21], considering the cost for graphite, ink, and the manufacturing. Material cost for MEA and delivery plates is proportional to their volume.

DESIGN INTEGRATION AND OPTIMIZATION

Design Objectives and Constraints

The design optimization considers both performances and costs of the fuel cell system. The performance measures include the United States Advanced Battery Consortium Dynamic Stress Test (USABC DST) efficiency [23][29], net power output, volumetric power density, and gravitational power density. The system cost measures include the operational cost, material cost, manufacturing cost and assembly cost. The fuel cell, as an engine for vehicles, has to fit within the given space of a passenger car. According to [24], the space is limited to $0.5\ m \times 1\ m^2$. In addition, the stack structural integrity is to be ensured.

Design Variables

The design optimization is carried out based on a given system gross power output of 64 kW and the operating current density 600 ASF. These conditions are chosen as in [20]. Based on these design conditions, a group of design variables are chosen as below:

Operational variable: the air stoichiometry, denoted by *airSt*;

Geometric dimensions of the stack and number of cells per stack:

- Stack width (assumed square cross-section), denoted by *stackW*,
- Supporting column width (assumed square cross-section), denoted by *colW*,
- Number of cells per stack, denoted by *nCell*,
- Height of the panel (fin), denoted by *finH*,
- Thickness of the stack end plate, denoted by *tEnd*, and
- Thickness of manifold covers, denoted by *tMani.*

Based upon a sensitivity study, the thickness of the endplate and the thickness of the manifolding cover are ruled out. These two variables only affect individual design objectives and behave independently to other design variables.

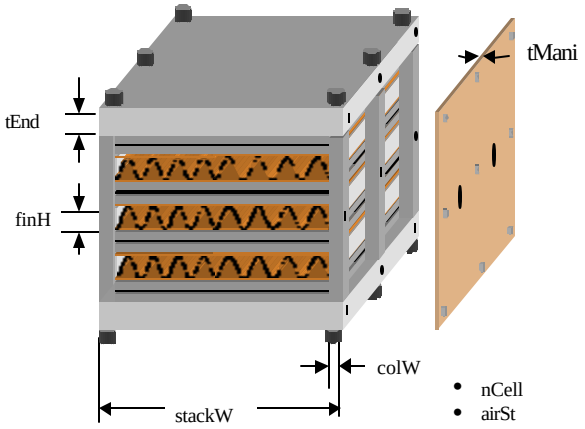

Fig. 2 TERS Stack Configuration and Chosen Design Variables

Design Optimization

Five variables: *airSt*, *stackW*, *colW*, *nCell*, and *finH* were chosen as the design variables, denoted as x_1, x_2, x_3, x_4, and x_5, respectively. A reference design, or base case, was chosen from [20] for design comparison, $\vec{x} = [2, 177.8, 19.05, 24, 9]$. A balanced functional performance and cost model is used first.

$$f(\vec{x}) = -\frac{1}{5}\sum_{i=1}^{5}(f_i - f_{i0})/f_{i0} \qquad (22)$$

where, f_i stands for function values (or life-cycle performance readings) of a given design, including the system USABC efficiency, net power output, two power densities, and the system cost; f_{i0} represents the function values for the base case. Equal weights are assigned to each of the design objectives. The resultant function value is a non-dimensional evaluation index considering all the design functions.

Based on the insights gained from the design exercises, the range limits for the five variables are set as in

Table 1, where the limits for the number of cells per stack are dependent on the system layout, which is discussed in the following section.

Table 1 Variable Ranges for TERS System Design

	Range
AirSt	1.3 ~ 2.5
StackW	100 ~ 240 mm
ColW	10 ~ 30 mm
NCell	10 ~ 130 mm (Layout (b)) or 10 ~ 60 mm (Layout (a))
FinH	4 ~ 15 mm

System Layout Comparison

The number of cells per stack is partially determined by the stack layout. Two possible stack layouts are illustrated in Fig. 3, given a fixed space. Intuitively, layout (b) can reduce the total number of stacks and present a better solution. This is to be verified through design optimization.

Optimization was carried out using ARSM through 88 function evaluations for both cases, with Layout (b) identified as the optimum.

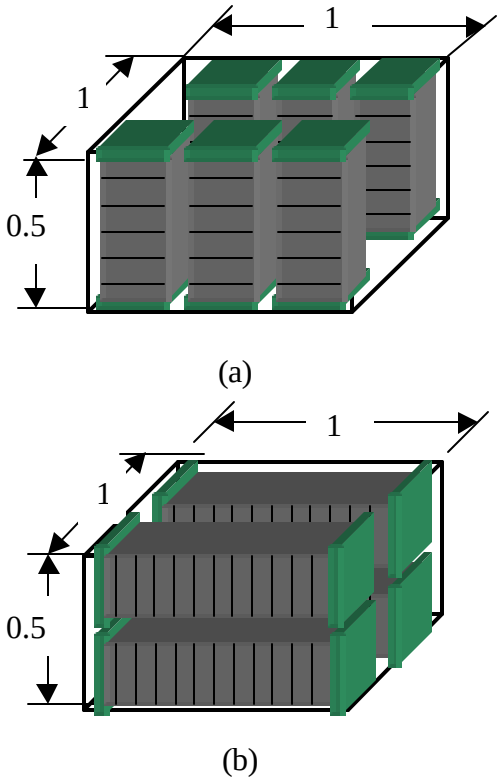

Fig. 3 Two Possible Spatial Layouts of Stacks

A comparison of the two layouts is given in

Table 2. Further design optimization was carried out on Layout (b).

Variable Sensitivity Analysis

One of the advantages of the RSM is that one can analyze the relative importance and interrelation between the design variables by comparing the coefficients of each term in the response function. For Layout (b) a sensitivity analysis was performed in the design space: xlv=[1.3 100 10 42 4]; xuv=[2.5 240 30 130 15] ('xlv' denotes the lower bound and the 'xuv' denotes the upper bound.).

With the normalized function in [-1 1] for all the variables, the response function is

$$\begin{aligned} f = {} & 3.141692 - 0.010491x_1 + 0.225782x_2 + 0.177225x_3 \\ & - 1.502814x_4 + 0.068936x_5 - 0.452034x_1^2 - 0.689531x_2^2 \\ & - 0.528705x_3^2 + 0.382227x_4^2 - 0.538712x_5^2 - 0.006670x_1x_2 \\ & + 0.000717x_1x_3 + 0.011240x_1x_4 - 0.000009x_1x_5 \\ & - 0.198845x_2x_3 + 0.202086x_2x_4 + 0.000252x_2x_5 \\ & - 0.129761x_3x_4 - 0.000094x_3x_5 + 0.00375x_4x_5 \end{aligned} \quad (23)$$

The normalized relative importance of each term is illustrated in Fig. 4. The horizontal coordinate indicates the sequence of terms as they appeared in the expression. Terms with negligible value are not shown. All terms are normalized with respect to the smallest coefficient.

The analysis shows air stoichiometry a less important variable and a week correlation between *airSt* and other variables. The value of air stoichiometry is chosen to be 2 based upon experiments. The analysis also shows a very week correlation between x_5, the fin height, and other design variables, although x_5 is a relatively important variable. The fin height is then assigned using its minimum value, 4 *mm*, to achieve better system power density and lower material cost.

Design Optimization on Other Variables

Three other design variables, panel height (*h*), number of cells per stack (*nCell*), and the stack width (*stackW*) are optimized next following two design scenarios. The first follows the same balanced performance and cost scenario, while the second follows the minimum cost design scenario that considers cost as design objective and functional performances as design constraints.

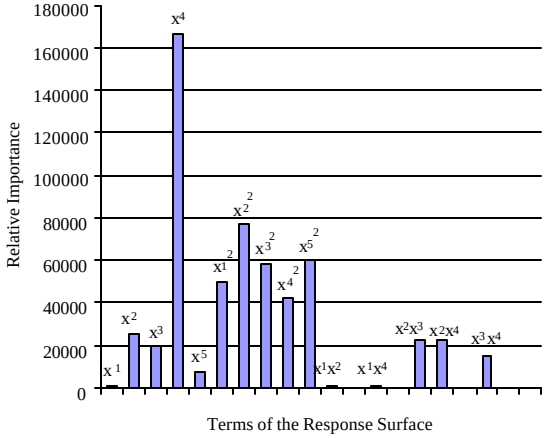

Fig. 4 Sensitivity of Each Term

Optimization results are given in Tables 3 and 4. The optimal design following Scenario I converged after only two search iterations (32 function evaluations), while the optimal design following Scenario II converged after nine iterations (144 function evaluations). Design improvements over the reference design or base case are illustrated in Table 5.

Within the constrained design space, the optimum following Scenario I presents a balanced performance and cost solution, while the optimum following Scenario II shows a minimum cost design at the sacrifice of system performance. Both design optima are superior to the reference design with improvements as much as 43 percent increase in power density and 16 percent reduction of system cost.

In the search of design optima, ARSM progressively approximates implicit and complex design objective and constraint functions through virtual prototyping. Through a limited number of design function evaluations, design optima with significant improvements are achieved within hours.

CONCLUSION

The method of modeling and evaluating the functional performances and costs of a complex mechanical system using mathematical models and virtual prototyping technique was discussed. A process of global design optimization based upon these evaluations and solved using the newly introduced ARSM scheme was presented. The method to model the functional performances and costs of a complex mechanical system was illustrated through the TERS transportation fuel cell system that involves complex electrochemical phenomena and heat/mass transfer processes. In the design optimization, seven design variables, both in continuous and discrete forms, are chosen to optimize the fuel cell system configuration. The optimization led to significant design improvements. In addition, the study also illustrated the capability and efficiency of the ARSM as a feasible design optimization tool for complex engineering design problems.

ACKNOWLEDGEMENT

Financial support from the Natural Science and Engineering Research Council of Canada, British Gas Canada and Ballard Power Systems, Inc., as well as technical assistance from Ballard and NGFT Research Laboratory staffs are gratefully acknowledged.

Professor **Behrouz Tabarrok** was a member of the first author's Ph.D. supervising committee. The authors would like to express their sincere appreciation to his valuable inputs and deep sorrow of losing a very respectable teacher and colleague.

REFERENCES

[1]. Amphlett, J. C., Baumert, R. M., Mann, R. F., Peppley, B. A., and Roberge P. R., 1995, "Performance Modeling of the Ballard Mark IV Solid Polymer Electrolyte Fuel Cell--I Mechanistic Model Development," *Journal of Electrochemistry Society*, Vol. 142, No. 1, pp. 1-8.

[2]. Angster, S., *et al.*, 1996, "Using VR for Design and Manufacturing Applications – A Feasibility Study," *Proceedings of the 1996 ASME Design Engineering Technical Conferences and Computers in Engineering Conference*, Irvine, California, August 18-22.

[3]. Box, G. E. P., and Hunter, J. S., 1957, "Multifactor Experimental Designs for Exploring Response Surfaces," *Annals of Mathematical Statistics*, 28, pp. 195-241.

[4]. Chen, W., 1995, *A Robust Concept Exploration Method for Configuring Complex System*, Ph.D. Thesis, Georgia Institute of Technology.

[5]. Doolittle, J. S., 1984, *Thermodynamics for Engineers*, John Wiley and Sons, Inc.

[6]. Fletcher, R., 1987, *Practical Methods of Optimization*, Second Edition, John Wiley & Sons, Ltd., New York, USA.

[7]. Grossmann, I. E., (ed.), 1996, *Global Optimization in Engineering Design*, Kluwer Academic Publishers.

[8]. Gupta, R., 1996, "Survey on Use of Virtual Environments in Design and Manufacturing," *Proceedings of the 1996 ASME Design Engineering Technical Conferences and Computers in Engineering Conference*, Irvine, California, August 18-22.

[9]. Haftka, R., Scott, E. P., and Cruz, J. R., 1998, "Optimization and Experiments: A Survey," *Applied Mechanics Review*, Vol. 51, No. 7, pp. 435-448.

[10]. Horst, R., and Tuy, H., 1990, *Global Optimization: Deterministic Approaches*, Springer-Verlag, Berlin.

[11]. Jones, D. R., et al., 1993, "Lipschitzian Optimization Without the Lipschitz Constant," Journal of Optimization Theory and Application, Vol. 79, No. 1, pp. 157-181.

[12]. Khuri, A. I., 1996, "Response Surface Models with Mixed Effects," *Journal of Quality Technology*, pp. 177-186.

[13]. Khuri, A. I., Cornell, J. A., 1987, *Response Surfaces: Design and Analyses*, Marcel Dekker, Inc.

[14]. Kim, J., Lee, S., and Sirinivasan, S., 1995, "Modeling of Proton Exchange Membrane Fuel Cell Performance with an Empirical Equation," *J. Electrochemistry Soc.*, Vol. 142, No. 8, pp.2671-2674.

[15]. Korngold, J. C., and Gabriele, G. A., 1997, "Multidisciplinary Analysis and Optimization of Discrete Problems Using Response Surface Methods," *Journal of Mechanical Design*, Vol. 119, pp. 427-433.

[16]. Li, X., 1996, *Course Notes on Fuel Cells*, Mechanical Engineering, University of Victoria.

[17]. Mistree, F., Patel B., and Vadde, S., 1994, "On Modeling Multiple Objectives and Multi-Level Decisions in Concurrent Design," *Advances in Design Automation*, ASME, Vol. 2, DE-Vol. 69-2, pp. 151-161.

[18]. Montgomery, D., 1991, *Design and Analysis of Experiments*, John Wiley and Sons, New York.

[19]. Myers, R. H., 1971, *Response Surface Methodology*, Allyn and Bacon, Inc.

[20]. Pastula, M., 1997, *Radiator Stack PEM Fuel Cell Architecture, System Modeling and Flow Field Design*, Master Thesis, University of Victoria.

[21]. Perry, M. L., 1997, Screen-Printing of Fuel and Oxidant Delivery Plates: A Low Cost manufacturing Alternative, Master thesis, University of Victoria.

[22]. Renaud, J. E., and Watson, L. T., 1998, "Convergence of Trust Region Augmented Lagrangian Methods Using Variable Fidelity Approximation Data," *Structural Optimization 15*, pp. 141-156.

[23]. Ronne, J., and Podhorodeski, R., 1996, "An Integrated Cost-Performance Model of a Transportation Solid Polymer Fuel Cell System," *Proceeding of the 2nd International Fuel Cell Conference*, pp.385-388.

[24]. Steinbugler, M, and Ogden, J., 1994, "Design Considerations for Proton Exchange Membrane Fuel Cells in Vehicles," *Abstract in the Proceedings of the 1994 Fuel Cell Seminar*, San Diego, California.

[25]. Suh, N. P., 1990, *The Principles of Design*, Oxford University Press.

[26]. Torczon, V., and Trosset, M., 1998, "Using Approximations to Accelerate Engineering Design Optimization," *Proceedings of the 7th AIAA/USAF/NASA/ISSMO Symposium on Multidisciplinary Analysis and Optimization*, St. Louis, pp. 738-401.

[27]. Wang, G., 1999, A Quantitative Concurrent Engineering Design Method Using Virtual Prototyping-Based Global Optimization and Its Application in Transportation Fuel Cells, Ph.D. Dissertation, University of Victoria.

[28]. Wang, G., Dong, Z., Pastula, M., and Kratschmar, K., "Virtual Prototyping-based Optimal Design of Multiple Function Panels for a New PEM Fuel Cell Stack," *Proceedings of the Design Automation Conference, the 1999 ASME Design Engineering Technology Conference*, Las Vegas, September 1999.

[29]. Xue, D., and Dong, Z., 1997, "Optimal Fuel Cell System Design Considering Functional Performance and Production Costs," *Proceedings of the 1997 ASME Design Engineering Technical Conferences*, September 14-17, Sacramento, California, DETC97/DAC-3971.

[30]. Z. Dong, and G. Wang, 1999, "Global Optimization of Mechanical Designs Based Upon Integrated Computer Models and Virtual Prototypes," *Integration of Process Knowledge into Design Support Systems*, Kluwer Academic Publishers, H. Kals and F. v. Houten (Eds.), pp. 309-320.

Table 2 A Comparison of the Two Different System Layouts

Layout	Efficiency (%)	Net Power (kw)	Power Density (w/l)	Power Density (w/kg)	System Cost Reduction (%)	Length (m)	Space (m^2)
(a)	53.345	57.249	171.427	137.323	7.172	0.499	0.27
(b)	54.163	57.453	173.328	143.051	11.527	0.998	0.14
Base	46.3	51.0	121.2	100.1	0	0.33	0.84

Table 3 Optimization Results for Balanced Performance and Cost Design (Scenario I)

Design Iteration	Design Space	Obtained Optimum	Function Index
1	xlv=[100 10 10] xuv=[240 30 114]	[140 10 114]	-0.210
2	Xlv=[100 10 10] xuv=[198 30 114]	[100 10 114]	-0.235

Table 4 Optimization Results for Minimum Cost Design (Scenario II)

Design Iteration	Design Space	Obtained Optimum	Percent Cost Lowered (%)
1	xlv=[100 10 10] xuv=[240 30 114]	[156 10 114]	14.978
2	xlv=[100 10 10] xuv=[235 30 114]	[154 10 114]	15.180
3	xlv=[111 10 10] xuv=[209 30 114]	[111 10 114]	14.406
4	xlv=[111 10 60] xuv=[209 30 114]	[147 10 114]	15.733
5	xlv=[111 10 60] xuv=[193 22 114]	[142 10 114]	15.982
6	xlv=[111 10 60] xuv=[181 17 114]	[139 10 114]	16.071
7	xlv=[111 10 60] xuv=[172 17 114]	[138 10 114]	16.091
8	xlv=[111 10 60] xuv=[170 15 114]	[137 10 114]	16.105
9	xlv=[130 10 105] xuv=[146 15 114]	[135 10 114]	16.120

Table 5 Design Improvements over the Reference (Base) Design

Designs	Efficiency Increase (%)	Net Power Increase (%)	Volumetric Power Density Increase (%)	Gravi-metric Power Density Increase (%)	System Cost Lowered (%)
Scenario I	12.02	6.20	43.49	43.49	12.07
Scenario II	6.09	3.83	40.59	40.75	16.12